

The nuclear spin-lattice relaxation rate in the PuMGa₅ materials

Yunkyu Bang

*Department of Physics, Chonnam National University, Kwangju 500-757,
and Asia Pacific Center for Theoretical Physics, Pohang 790-784, Korea*

M. J. Graf, N. J. Curro, and A. V. Balatsky

Los Alamos National Laboratory, Los Alamos, New Mexico 87545, USA

(Dated: March 23, 2022)

We examine the nuclear spin-lattice relaxation rates $1/T_1$ of PuRhGa₅ and PuCoGa₅, both in the superconducting and normal states, as well as their Knight shifts. Results for both compounds are consistent with a superconducting gap of d-wave symmetry in the presence of strong impurity scattering, though with quite different gap-over- T_c ratios $2\Delta_0/k_B T_c$ (8 for PuCoGa₅ and 5 for PuRhGa₅). In the normal state, PuRhGa₅ exhibits a gradual suppression of $(T_1 T)^{-1}$ below 25 K, while measurements for PuCoGa₅ reveal a monotonic increase down to T_c . We propose that this behavior is consistently understood by the crossover from the two-dimensional quantum antiferromagnetic regime of the local 5*f*-electron spins of Pu to the concomitant formation of the fermion pseudogap based on the two-component spin-fermion model.

PACS numbers: 74.20.74.20-z, 74.50

I. INTRODUCTION

The discovery of superconductivity (SC) in plutonium based systems such as PuCoGa₅ and PuRhGa₅ has stimulated the study of unconventional superconductivity and the pairing symmetry and mechanism in these materials.^{1,2} The symmetry of an unconventional superconductor is reduced compared to the symmetry of its normal state, thus resulting in many novel properties of the quasiparticle excitation spectrum. With a record high superconducting transition temperature T_c of the order of 20 K among the 4*f* and 5*f* electron based compounds, this class of materials provides hope for a unifying pairing mechanism from heavy fermion superconductors to the high- T_c cuprates.^{3,4} It is believed that the superconducting action in Pu-115 [PuMGa₅ with $M=\text{Co}$ and Rh] derives itself from the unique character of the 5*f* electrons of plutonium.⁴ PuMGa₅ is isostructural to the tetragonal Ce-115 series [CeMIn₅]. Very recently, Curro and coworkers³ proposed, based on their measurements of the Knight shift and spin-lattice relaxation rates, that the Pu-115 compounds are bridging the superconducting and normal-state properties of the heavy-fermion Ce-115 and high-temperature copper-oxide superconductors. Therefore providing a means for tuning the interaction strength of antiferromagnetic spin fluctuations to intermediate values between both extreme limits.⁵

In this paper, we examine the spin-lattice relaxation rates T_1^{-1} of PuCoGa₅ and PuRhGa₅ in the superconducting and normal states. Very recently, Sakai and coworkers⁶ have measured T_1^{-1} in PuRhGa₅ in the superconducting state and found evidence for lines of nodes in the gap function, just as in PuCoGa₅, but with a much reduced superconducting transition temperature $T_c \approx 8.5$ K versus $T_c \approx 18.6$ K. Both materials differ primarily in their lattice parameters, since Rh has a slightly larger atomic radius than Co.⁵ For example, the *ab* plane and *c* axis lattice constants are larger in PuRhGa₅ but the ratio *c/a* is larger in PuCoGa₅, suggesting that PuRhGa₅ is less two dimensional (2D). Predicting the consequences of this elongation on the superconducting instability is not

straightforward; however, we find that this small change of lattice constants leads to dramatic changes in the electronic and magnetic properties in this class of materials.

Here, we give a detailed theoretical description of the spin-lattice relaxation rate and predict what should be observed if the Knight shift was measured on the same sample. Our self-consistent treatment of impurity scattering in the superconducting state goes beyond the two-fluid approach used by Sakai et al.⁶, which was used to explain the large residual density of states in PuRhGa₅. Further, our theoretical fits to the experimental data of PuRhGa₅ lead us to three important conclusions: First, the measured pair-breaking effect of impurities in PuRhGa₅ reduces the transition temperature of a hypothetically pure sample by only 0.5 K. Therefore, the lower T_c of PuRhGa₅ is an intrinsic property and is not due to impurities. Second, the theoretical fits indicate that the ratio $2\Delta_0/k_B T_c$ is markedly reduced in PuRhGa₅ (~ 5) versus PuCoGa₅ (~ 8). This fact indicates that the mediating bosonic pairing glue is stronger in PuCoGa₅. Assuming that Pu-115 compounds are spin-fluctuation mediated superconductors,⁴ we conclude that Rh substitution reduces the strength of the mediating spin fluctuations. Indeed, this conclusion is supported by the observed behavior of $1/T_1$ in the normal state of both compounds. Third and most interestingly, when the experimental data are plotted as $T_1 T$ versus T , we find that in the normal state $T_1 T$ of PuRhGa₅ saturates and is nearly flat over a wide temperature region $T_c < T < 3T_c$, whereas $T_1 T$ in PuCoGa₅ shows a monotonic decrease down to T_c . This saturation resembles closely the pseudogap (PG) feature of the underdoped cuprates.⁷ As a possible explanation of this phenomenon, we propose the two-component spin-fermion model of antiferromagnetically correlated metals⁸ and argue that the two natural energy gaps accounting for the PG behavior in Pu-115 are the spin gap Δ_{SG} and the fermion gap Δ_{FG} .

II. SUPERCONDUCTING STATE

The experimental techniques of nuclear magnetic resonance (NMR) and nuclear quadrupolar resonance (NQR) have been used successfully in the past to distinguish between the spin states of Cooper pairs (spin singlet vs. spin triplet pairing) and provide indirect information on the symmetry of the gap function – fully gapped vs. nodal lines or nodal points in the gap function on the Fermi surface. Both techniques probe directly the quasiparticle density of states and reveal indirect information about the pairing symmetry.

The standard explanation of power vs. exponential laws in the low-temperature behavior of thermodynamic and transport properties, for example, the spin-lattice relaxation rate $1/T_1$, comes from the difference of nodal and fully gapped excitation spectra in the superconducting state. In clean nodal superconductors $1/T_1$ exhibits a nearly T^3 behavior far below the superconducting transition temperature, $T \ll T_c$, while it is exponential for gapped superconductors. On the other side, deviations from this behavior, like the T -linear temperature dependence of $1/T_1$ at low temperatures, are explained by impurity effects in an unconventional superconductor with lines of nodes on the Fermi surface.

In our calculations the effect of impurity scattering is included within the self-consistent T -matrix approximation,⁹ which is the standard formulation for pointlike defects in a superconducting dilute alloy.^{10,11,12} For the case of particle-hole symmetry of the quasiparticle excitation spectrum the Nambu component T_3 of the T matrix vanishes, and for a d-wave order parameter with isotropic scattering $T_1 = 0$ (also without loss of generality we can choose $T_2 = 0$ by general U(1) gauge symmetry), where T_i is the i th component of the 2×2 Nambu matrix expanded in Pauli matrices. Then we need to calculate only $T_0(\omega)$. The impurity self-energy is given by $\Sigma_0 = \Gamma T_0$, where $\Gamma = n_i/\pi N_0$. Here N_0 is the normal density of states (DOS) at the Fermi surface, n_i is the impurity concentration; $T_0(\omega_n) = \frac{g_0(\omega_n)}{[c^2 - g_0^2(\omega_n)]}$, where $g_0(\omega_n) = \frac{1}{\pi N_0} \sum_k \frac{i\tilde{\omega}_n}{\tilde{\omega}_n^2 + \varepsilon_k^2 + \Delta^2(k)}$. The impurity renormalized Matsubara frequency is defined by $\tilde{\omega}_n = \omega_n + \Sigma_0$, with $\omega_n = \pi T(2n+1)$, and the scattering strength parameter c is related to the s-wave phase shift δ_0 by $c = \cot(\delta_0)$. Using this self-energy Σ_0 the following gap equation is solved self-consistently,

$$\Delta(\phi) = -N_0 \int \frac{d\phi'}{2\pi} V(\phi - \phi') \times T \sum_{\omega_n} \int_{-\omega_c}^{\omega_c} \frac{d\varepsilon \Delta(\phi')}{\tilde{\omega}_n^2 + \varepsilon^2 + \Delta^2(\phi')}, \quad (1)$$

where $V(\phi - \phi')$ is the angular parameterization of the pairing interaction, and ω_c is a typical cutoff energy. We assume the canonical d-wave gap function of the form $\Delta(\vec{k}) = \Delta_0(\cos k_x - \cos k_y)$ or $\Delta(\phi) = \Delta_0 \cos(2\phi)$ for a cylindrical Fermi surface. The pairing potential $V(\phi - \phi')$ induces a gap with d-wave symmetry. Although its microscopic origin is not the issue of this paper, we believe it originates from 2D antiferromagnetic (AFM) spin fluctuations. The static limit of the spin suscep-

tibility of the AFM fluctuations, $\chi(\mathbf{q}, \omega = 0) \sim \frac{1}{(\mathbf{q} - \mathbf{Q})^2 + \xi^{-2}}$, is parameterized near the AFM wave vector \mathbf{Q} as⁸

$$V(\phi - \phi') = V_d(b) \frac{b^2}{(\phi - \phi' \pm \pi/2)^2 + b^2}, \quad (2)$$

where the parameter b is inverse proportional to the AFM correlation length ξ , normalized by the cylindrical Fermi surface ($\xi \sim a\pi/b$; a is the lattice parameter). For all calculations in this paper, we choose $b = 0.5$ which is not a sensitive parameter for our results unless ξ is very large ($b < 0.1$),⁸ i.e., within the range of $0.1 < b < 1$ our results show little variations and are qualitatively the same.

With the gap function $\Delta(\phi)$ and $T_0(\omega)$ obtained from Eq. (1) (where $T_0(\omega)$ is analytically continued from $T_0(\omega_n)$ by Padé approximation) we calculate the nuclear spin-lattice relaxation rate $1/T_1$ following the standard formulation^{3,9,10}

$$\frac{1}{T_1 T} \sim - \int_0^\infty \frac{\partial f_{FD}(\omega)}{\partial \omega} \left[\left\langle \text{Re} \frac{\tilde{\omega}}{\sqrt{\tilde{\omega}^2 - \Delta^2(\phi)}} \right\rangle_\phi^2 + \left\langle \text{Re} \frac{\Delta(\phi)}{\sqrt{\tilde{\omega}^2 - \Delta^2(\phi)}} \right\rangle_\phi^2 \right], \quad (3)$$

and the superconducting spin susceptibility χ_s

$$\frac{\chi_s}{T} \sim - \int_0^\infty \frac{\partial f_{FD}(\omega)}{\partial \omega} \left\langle \text{Re} \frac{\tilde{\omega}}{\sqrt{\tilde{\omega}^2 - \Delta^2(\phi)}} \right\rangle_\phi, \quad (4)$$

where $f_{FD}(\omega)$ is the Fermi-Dirac function, the impurity renormalized quasiparticle energy $\tilde{\omega} = \omega + \Sigma_0(\omega)$, and $\langle \dots \rangle_\phi$ means the angular average over the Fermi surface. The first term in the bracket of Eq. (3) is $N^2(\omega)$. The second term vanishes in our calculations because of the symmetry of the gap function. To calculate $1/T_1 T$ using Eq. (3), or χ_s using Eq. (4), we need the full temperature dependent gap function $\Delta(\phi, T)$ and T_c . Our gap equation Eq. (1) is the BCS gap equation, therefore it gives the BCS temperature behavior for $\Delta(\phi, T)$ and $\Delta_0 = 2.14 k_B T_c$ for the standard weak-coupling d-wave SC. In order to account for strong-coupling effects we use the phenomenological formula $\Delta(\phi, T) = \Delta(\phi, T = 0) \Xi(T)$ with $\Xi(T) = \tanh(\beta \sqrt{T_c/T - 1})$, and parameters β and Δ_0/T_c . Then we only need to calculate $\Delta(\phi, 0)$ at zero temperature. The temperature dependence of $\Sigma_0(\omega, T) \equiv \Gamma T_0(\omega, T)$ is similarly extrapolated: $T_0(\omega, T) = T_0(\omega, T = 0) \Xi(T) + T_{normal}(1 - \Xi(T))$, where $T_{normal} = \Gamma/(c^2 + 1)$ is the normal state T_0 . In our numerical calculations we chose $\beta = 1.74$, because our final results are not very sensitive with respect to this parameter, while the ratio $\Delta_0/k_B T_c$ is an important parameter to simulate strong-coupling effects. The larger the gap ratio the more important are strong-coupling effects.

In figures 1 and 2 the spin-lattice relaxation rate of PuRhGa₅ by Sakai et al.⁶ is shown. For ease of comparison $1/T_1$ was normalized to $1/T_1 = 10$ at $T = T_c$. The insets show the corresponding normalized quasiparticle DOS for varying scattering rates Γ . With our earlier described choice of gap parameters ($\beta = 1.74$ and $2\Delta_0 = 5 k_B T_c$) an impurity scattering

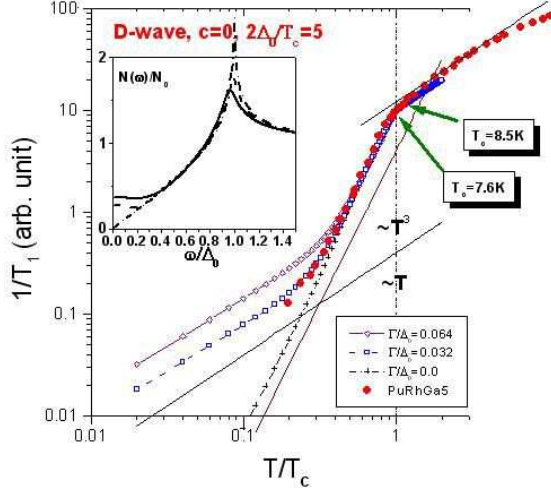


FIG. 1: The NQR spin-lattice relaxation rate⁶ plotted versus temperature normalized by the superconducting transition temperature $T_c = 7.6$ K. Calculations are shown for $2\Delta_0 = 5k_B T_c$ and three values of the impurity scattering rate Γ for unitary scattering. Inset: The normalized quasiparticle density of states is shown for corresponding values of the impurity scattering rate $\Gamma/\Delta_0 = 0, 0.032, 0.064$.

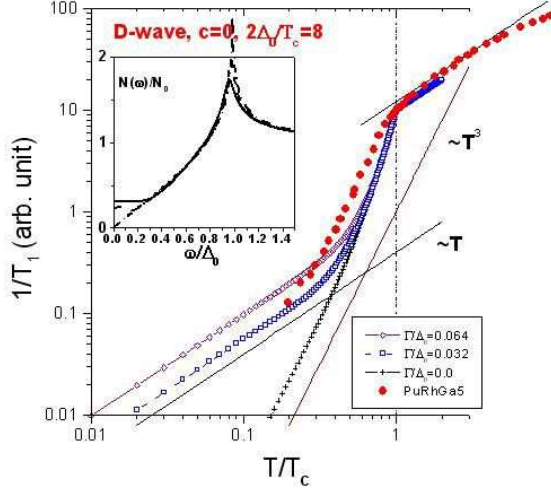


FIG. 2: The NQR spin-lattice relaxation rate⁶ plotted versus temperature normalized by the superconducting transition temperature $T_c = 7.6$ K. Calculations are shown for $2\Delta_0 = 8k_B T_c$ and three values of the impurity scattering rate Γ for unitary scattering. Inset: The normalized quasiparticle density of states is shown for corresponding values of the impurity scattering rate $\Gamma/\Delta_0 = 0, 0.032, 0.064$.

rate of $\Gamma/\Delta_0 = 0.032$ in the unitary limit ($c = 0$) is enough to completely fill the low energy gap with impurity states, where $N(\omega = 0)$ reaches more than 25% of the normal-state DOS N_0 . For a higher value of $\Gamma/\Delta_0 = 0.064$, the T -linear region extends up to $\sim 0.35 T_c$. At temperatures near T_c the coherence peak is almost invisible because of the sign-changing gap

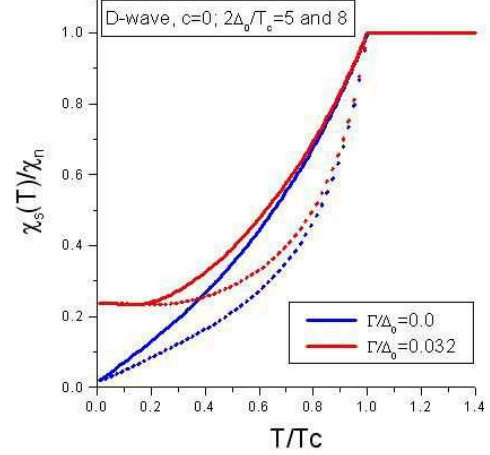


FIG. 3: The calculated spin susceptibility χ_S of a d-wave SC normalized by its normal state value χ_N for gap values $2\Delta_0 = 5k_B T_c$ (solid lines) and $8k_B T_c$ (dotted lines), and impurity scattering rates $\Gamma/\Delta_0 = 0$ and 0.032 .

function, i.e., vanishing of the second term in Eq. (3).

Below T_c the spin-lattice relaxation rate shows a nearly T^3 behavior until it crosses over to a T -linear region. A comparison with the experimental data by Sakai et al.⁶ is in good agreement with a scattering rate close to $\Gamma/\Delta_0 = 0.032$. Based on this value, we estimate the reduction of T_{c0} of a hypothetically pure sample due to impurities to be $T_{c0} - T_c = \frac{\pi}{4}\Gamma \approx 0.53$ K, which results in $T_{c0} \approx 8.1$ K or 9.0 K, depending on the value of $T_c = 7.6$ K or 8.5 K. This small suppression and large impurity induced DOS is a characteristic of unitary impurities ($c=0$).

In Fig. 1 we obtained a better fit to the experimental data (symbols) assuming a slightly lower superconducting transition temperature $T_c = 7.6$ K than the reported value of $T_c = 8.5$ K by Sakai et al.⁶ This could indicate the presence of a pseudogap similar to the high-temperature superconductor $\text{YBa}_2\text{Cu}_3\text{O}_{7-\delta}$, where $1/T_1$ is suppressed starting above T_c .

In Fig. 2, we plot $1/T_1$ for an enhanced strong-coupling d-wave gap of $2\Delta_0 = 8k_B T_c$, as was recently reported for PuCoGa_5 .³ Due to the larger gap value, the theoretical $1/T_1$ drops initially faster below T_c than the experimental data. Hence, we find a poorer fit to the measured data for this choice of strong-coupling gap. It demonstrates that the comparison of $1/T_1$ data with theoretical calculations is a useful tool for determining the strong-coupling gap value $\Delta_0/k_B T_c$.

Fig. 3 shows the prediction for the spin susceptibility, χ_S , or its corresponding NMR Knight shift, $K = K_0 + A\chi_S$, where K_0 and A are constants for most materials. χ_S is calculated for the same d-wave gap values as was used for the spin-lattice relaxation rates in figures 1 and 2. Again a modest impurity scattering rate of $\Gamma/\Delta_0 = 0.032$ results in a large residual susceptibility at zero temperature, equivalent to roughly 25% of the normal-state DOS or spin susceptibility χ_N . The quantitative difference in the spin susceptibilities between gap values

$2\Delta_0 = 5k_B T_c$ and $8k_B T_c$ should be easily discernible in future measurements of the Knight shift.

At first sight it might appear that the sample PuRhGa₅ had three times more defects than PuCoGa₅ of similar age, based on our best-fit scattering rates of $\Gamma/\Delta_0 = 0.032$ for PuRhGa₅ and $\Gamma/\Delta_0 = 0.01$ for PuCoGa₅. This could be explained by slightly different isotope mixes of plutonium used. However, if we express the scattering rates in absolute values, we find very similar impurity scattering rates for both samples, namely, $\Gamma = 0.6$ K for PuRhGa₅ and $\Gamma = 0.7$ K for PuCoGa₅, consistent with a common origin of defect generation due to self-irradiation by plutonium.

One final remark is warranted, namely, that the experimental data by Sakai et al. in Fig. 1 are normalized assuming a slightly lower superconducting transition temperature $T_c = 7.6$ K than the reported value by the authors. Indeed, if T was normalized by $T_c = 8.5$ K, then the fitting would be poorer and in particular the excess relaxation rate just below T_c could not be explained by a simple superconducting transition. The origin of this ambiguity of T_c is not clear at the moment. If the true T_c of the sample was indeed 7.6 K, as was used in Fig. 1, then the incorrectly assigned $T_c = 8.5$ K might be due to the presence of a pseudogap that will be discussed in the next section.

III. NORMAL STATE

Next we address the non-Fermi liquid behavior of the Pu-115 compounds in the normal state. As we will argue below, this behavior can be consistently understood within spin fluctuation theory. In Fig. 4(a), we plot the inverse of the measured $1/T_1$ for PuCoGa₅ and PuRhGa₅ multiplied by T versus temperature up to higher temperatures (multiple times T_c). A Fermi liquid should exhibit a constant $T_1 T$ in the normal state, in contrast to the succinct features of Pu-115: (1) at high temperatures ($T \gtrsim 25$ K) both data show T -linear behavior; (2) $T_1 T$ in PuCoGa₅ shows monotonic decrease down to T_c — a small deviation from the T -linear behavior in the region of $T_c \lesssim T \lesssim 30$ K calls for additional explanation; (3) the most interesting feature of the curve is the gradual round-off of $T_1 T$ in the PuRhGa₅ data below ~ 20 K. Even the superconducting transition at $T_c = 8.5$ K or 7.6 K is not clearly discernible from these data. This roundoff in $1/T_1 T$ starting far above T_c has been frequently observed in underdoped high temperature superconductors and has been attributed to the suppression of low-energy spin fluctuations associated with the pseudogap behavior. Recently, experiments of several heavy fermion compounds showed such a pseudogap behavior.^{13,14} While the pseudogap behavior in heavy fermions typically shows only in a very narrow temperature range of a few Kelvin, it provides a much clearer evidence for its magnetic origin than in the cuprates. For the cases of CeIn₃ and CeRhIn₅^{14,15} the pseudogap occurs in NMR data above the Néel temperature T_N . In addition, the pseudogap of CeCoIn₅ occurs above the superconducting transition, a system which is known to be very close to the two-dimensional antiferromagnetic quantum criticality (QC).¹³

Considering that Pu-115 materials are near a 2D antiferromagnetic (AFM) instability, we start with the phenomenological model of the antiferromagnetically correlated metal. The minimal set of low energy degrees of freedom are the fermionic charge excitations and the collective spin excitations. This phenomenological theory is also called spin-fermion model and has been intensively studied by Pines and coworkers.¹⁶ In contrast to this standard spin-fermion model, we proposed for heavy fermions the two-component spin-fermion model,⁸ where the spin modes originate directly from localized spins rather than from collective particle-hole excitations. In a mixed momentum and real-space representation the corresponding Hamiltonian is written as

$$H = \sum_{\mathbf{k}, \alpha} c_{\alpha}^{\dagger}(\mathbf{k}) \epsilon(\mathbf{k}) c_{\alpha}(\mathbf{k}) + \sum_{\mathbf{r}, \alpha, \beta} \vec{J}(\mathbf{r}) \cdot c_{\alpha}^{\dagger}(\mathbf{r}) \vec{\sigma}_{\alpha\beta} c_{\beta}(\mathbf{r}) + H_S \quad (5)$$

where the first term is the fermionic kinetic energy and the second term describes the coupling between local spins $\vec{S}(\mathbf{r})$ and the spin density of the conduction electrons. The last term represents an effective low-energy Hamiltonian for the local spins. When the local spins have a short range AFM correlation, the spin correlation function has the general form¹⁷

$$\chi(\mathbf{q}, \omega) = \frac{\chi(\mathbf{Q}, 0)}{1 + \xi^2 |\mathbf{q} - \mathbf{Q}|^2 - \omega^2 / \Delta_{SG}^2 - i\omega / \bar{\omega}}, \quad (6)$$

where Δ_{SG} is the spin gap, \mathbf{Q} the 2D AFM ordering vector, ξ the magnetic correlation length, and $\bar{\omega}$ the spin relaxation energy scale, which comes from Landau damping of the fermionic sector. Given the above form of the spin susceptibility $\chi(\mathbf{q}, \omega)$ and assuming the 2D AFM correlation¹⁸, it has been shown that $1/T_1 T \sim 1/\bar{\omega}$.¹⁹ Further, it is known that $\bar{\omega} \sim \xi^{-1}$ for the $z=1$ quantum-critical phase of the 2D quantum antiferromagnet.²⁰ As was shown by Chakravarty and coworkers,²⁰ the magnetic correlation length displays, depending on the phases of quantum criticality (QC) or quantum disorder (QD) the following behavior:

$$\xi^{-1} \sim \begin{cases} T & \text{for QC } (T > T^*) \\ \text{const.} & \text{for QD } (T < T^*) \end{cases} \quad (7)$$

The high-temperature T -linear behavior in $T_1 T$, see Fig. 4(a), of PuCoGa₅ and PuRhGa₅ can be understood as a generic feature of the quantum critical regime of the 2D Heisenberg antiferromagnet.²⁰ In principle, this high temperature QC explanation can be tested by the measurement of the spin-spin relaxation time T_{2G} , as was done for the high-temperature superconductors;²¹ then the simple relation $T_1 T / T_{2G}^z = \text{const.}$ should characterize the QC dynamics in Pu-115 by determining the dynamic critical exponent z . Also the low-temperature round-off in $T_1 T$ of PuRhGa₅ can be associated with the QC to QD crossover of the 2D AFM. However, it is still not sufficient to explain the additional fall-off of $1/T_1 T$ between 20 K and $T_c \approx 7.6$ K (for more detail see the inset of Fig. 4(b)). We propose that this additional suppression of the spin-fluctuations is caused by the suppression of the fermionic DOS (namely the fermionic pseudogap). Since the term $i\omega/\bar{\omega}$ in Eq.(6) originates from Landau damping of the fermionic

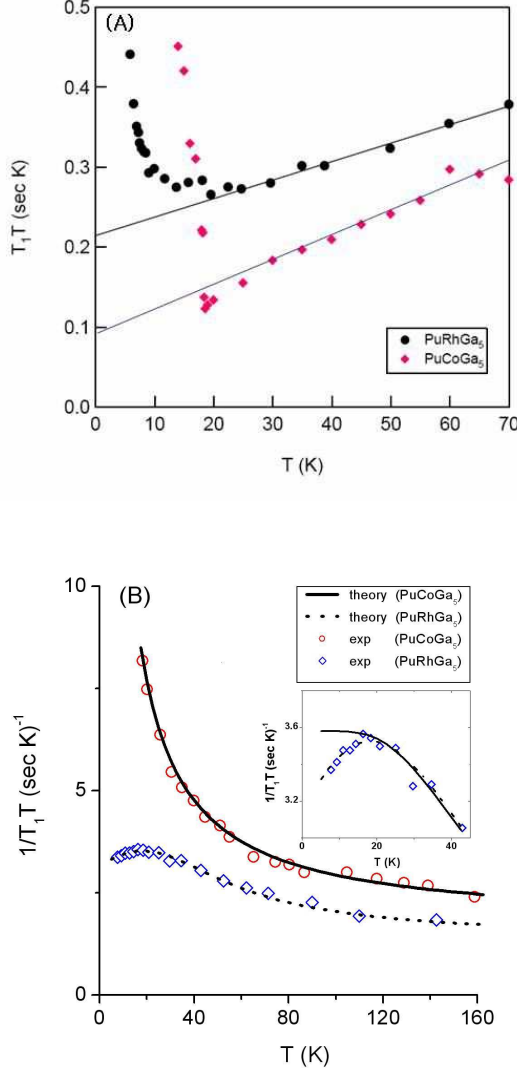


FIG. 4: (a) Plot of T_1T data vs. T of PuCoGa₅ and PuRhGa₅. (b) Plot of $1/T_1T$ vs. T for a wider temperature range of the normal state for PuRhGa₅ (open diamonds) and PuCoGa₅ (open circles) and the theoretical fits. Parameters for the theoretical fits are $\Delta_{SG}=20$ K and $\Delta_{FPG}=8$ K for PuRhGa₅ and $\Delta_{SG}=0$ K and $\Delta_{FPG}=8$ K, respectively. Inset: Close-up view for PuRhGa₅ at low temperatures. Theoretical fits with (dotted line) and without (solid line) the fermionic PG correction are shown for comparison. (PuRhGa₅ data are from Ref.[6].)

sector, instead one needs to include $\sim i\omega N(E_F, T)/\bar{\omega}$. Therefore, when the fermionic DOS $N(E_F)$ becomes temperature dependent, it needs to be included and leads to the modification $1/T_1T \sim N(E_F, T)/\bar{\omega}(T)$.

Several authors²² have studied the influence of magnetic correlations on fermionic quasiparticles and found that increasing the magnetic correlation length ξ causes a precursor effect of a spin-density wave state, which forms a quasi-gap in the DOS. The amount of the suppression of the DOS depends sensitively on the parameters, such as the size of the correlation length ξ , the coupling constant, and temperature, etc.

In this paper, therefore, we merely introduce a phenomenological form of the pseudo-gapped DOS, $N(E_F, T, \Delta_{FPG})$. The systematic numerical studies of the fermionic pseudo-gap (FPG) Δ_{FPG} due to magnetic correlation in the two-component spin-fermion model will be reported elsewhere.

Combining the temperature dependence of the FPG and the magnetic correlation of the 2D AFM, we can write $1/T_1T$ in the two-component spin-fermion model as

$$\frac{1}{T_1T} = AN_0(E_F)[1 - \tanh^2(\frac{\Delta_{FPG}}{2\sqrt{T^2 + \Gamma^2}})] \times \frac{1}{[\Delta_{SG} + T \exp(-4\Delta_{SG}/T)]} + B. \quad (8)$$

The first factor $N_0(E_F)[1 - \dots]$ is the phenomenological form of the fermionic DOS with FPG Δ_{FPG} and damping rate Γ . The second factor $\frac{1}{[\Delta_{SG} + \dots]}$ is a smooth crossover function²⁰ for $\xi(T)$ describing the QC to QD behavior of Eq.(7) with the spin gap $\Delta_{SG} \sim T^*$. Here, B is a constant describing a temperature independent contribution and A is a constant scale factor. Using this formula, we fit the experimental data of PuCoGa₅ and PuRhGa₅ for normal state in Fig. 4(b). The fitted results are in excellent agreement with experiment, where the two key fitting parameters provide estimates for the important energy scales of this phenomenological model. For PuRhGa₅, we used $\Delta_{SG} = 20$ K and $\Delta_{FPG} = 8$ K; the damping rate Γ is not a very sensitive model parameter, so we use $\Gamma=25$ K in all cases. A spin gap of $\Delta_{SG} \sim T^* = 20$ K can be read off from the data in Fig. 4(a), where T_1T deviates from a linear temperature dependence. However, notice that without the FPG correction Δ_{FPG} the additional drop of $1/T_1T$ in the region of $T_c < T < T^*$ cannot be explained only by the QC to QD crossover of ξ , see the inset of Fig. 4(b). For PuCoGa₅, the monotonically increasing $1/T_1T$ at lower temperatures implies increasing $\xi(T)$ and stronger magnetic correlations than in PuRhGa₅. Along the same line of thought, as applied to PuRhGa₅, the FPG should also be formed in the case of PuCoGa₅. In Fig. 4(b), we used $\Delta_{SG} = 0$ K and $\Delta_{FPG} = 8$ K for PuCoGa₅. The FPG effect is not much visible because it is overwhelmed by the stronger temperature dependence of $1/\bar{\omega} \sim \frac{1}{T}$ for PuCoGa₅. For PuCoGa₅, we could obtain a same quality of good fits with different values of Δ_{FPG} as large as ~ 20 K.

We summarize the effects of the magnetic correlations in PuCoGa₅ and PuRhGa₅ on the thermodynamic behavior in the schematic phase diagram in Fig. 5 with respect to a generic coupling parameter g . The assignment of PuCoGa₅ rather than PuRhGa₅ to the vicinity of the quantum critical point (QCP) in the QC region is consistent with various other experiments: for instance, the lower T_c , the smaller the value of the specific heat jump $\Delta C/T_c \approx 45$ mJ mol⁻¹ K⁻²,²³ and the smaller the gap-over- T_c ratio $2\Delta_0/T_c$ in PuRhGa₅ compared to PuCoGa₅. Also the resistivity of PuCoGa₅ shows an anomalous power law dependence¹, $\rho \propto T^{4/3}$, as expected near a quantum phase transition. All these experimental data indicate that the 2D AFM fluctuations are weaker in PuRhGa₅ than in PuCoGa₅. In Fig. 5 we added the crossover line (thin dotted line) to the FPG region, T_{FPG} . The formation of the

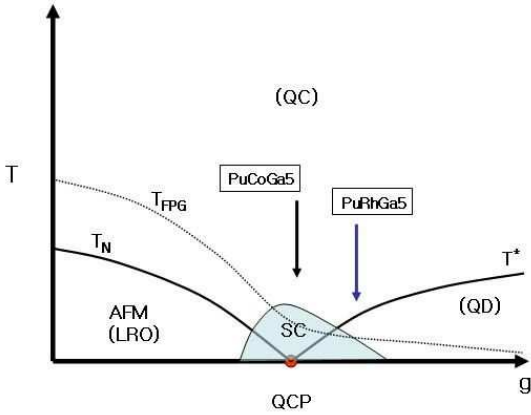


FIG. 5: The schematic phase diagram for the alloy system $\text{Pu}(\text{Co,Rh})\text{Ga}_5$. Thick solid lines are the 2D AFM transition temperature (T_N) and the QC to QD crossover temperature (T^*). The thin dotted line is the crossover temperature (T_{FPG}) to the fermionic pseudogap (FPG) region.

FPG is not a universal property and depends on material specific details. Nevertheless, in order to understand the detailed behaviors of $1/T_1T$ in PuMGa_5 materials, it is indispensable to be included.

To complete our discussion, we briefly describe possibility of alternative explanations. In recent Knight shift (K) measurements in PuRhGa_5 , Sakai et al.²⁴, found that the Knight shift failed to track the bulk susceptibility (χ) below a temperature $\sim 30\text{K}$. Such K - χ anomaly is known to exist in other heavy fermion compounds and various explanations were proposed²⁵. Naturally this anomaly is likely to be related to the anomalous temperature dependence of T_1 ²⁶; however, the deviation of $K \propto \chi$ relation *per se* doesn't necessarily mean the suppression of $1/T_1T$. There are three proposals for K - χ anomaly in the literature: (1) CEF (crystal effective fields)²⁷: the population of different CEF levels of f-electron changes with temperature and hence the HF (hyperfine) coupling between nuclei spin and the f-electron spin obtains a temperature dependence. (2) Kondo cloud screening²⁸: the HF coupling between nuclei spin and the f-electron spin is mediated by the RKKY modulation of the conduction electrons. The onset of Kondo screening would change the characteristics of the RKKY modulation and leads to the change of HF coupling. (3) Two fluids model²⁵: total susceptibility consists of two part – one from f-electrons and the other from conduction electrons – and each component has different temperature dependence and HF couplings to the nuclei spin. Due to the different temperature dependence of each susceptibility, the non-proportionality between K and χ can be explained.

The proposals (1) and (2) are basically invoking on the temperature dependent HF coupling but by different mechanisms: Kondo and CEF, respectively. Our model is similar to the pro-

posal (3) in the spirit of the two fluids model. However, there are technical and conceptual differences between (3) and our model. First, technical difference is the following. While we also assume two susceptibilities – one from local f-electron and the other from conduction electron, our two fluids model is not a simple addition of two susceptibilities. We assume that the dominant contribution (the interesting temperature dependent part) always comes from the local f-electrons. But the f-electron susceptibility essentially obtains its low energy dynamics through coupling with the conduction electrons and as a result the conduction electron susceptibility always feeds back into the f-electron susceptibility and vice versa (see $i\omega/\bar{\omega}$ term in Eq.(6)). Second, the most important conceptual difference is that we assume that the temperature dependence of the f-electron susceptibility for the range of interesting temperatures is arising from a magnetic correlation of local f-electrons but not from Kondo or CEF effect. This point of departure is very crucial and should be determined by experiments. There are already abundant experimental evidences that CeM ($M = \text{Co, Rh, Ir}$) In_5 materials are inside or in the vicinity of AFM ordered phase²⁹. For PuM ($M = \text{Co, Rh}$) Ga_5 , there are yet no direct measurements of the magnetic correlations, but the fact of a D-wave pairing³ in the superconducting state and the anomalous temperature dependence of dc-resistivity⁴ indicate that PuMGa_5 materials are near AFM instability as sketched in Fig.5.

IV. CONCLUSION

We have studied the nuclear spin-lattice relaxation rates $1/T_1$ of PuCoGa_5 and PuRhGa_5 , both in the normal and superconducting states. In the superconducting state, both compounds display the features of a dirty d-wave superconductor with impurity scattering in the unitary limit. This also is borne out in the calculated Knight shifts. The superconducting gap values of $2\Delta_0/T_c$ are ~ 8 and ~ 5 for PuCoGa_5 and PuRhGa_5 , respectively, indicating that pairing fluctuations are much stronger in PuCoGa_5 than in PuRhGa_5 .

In the normal state, the temperature behavior of $1/T_1$ between both compounds is qualitatively different at low temperatures. While $1/T_1T$ of PuCoGa_5 displays a genuine quantum-critical behavior similar to a 2D quantum antiferromagnet down to T_c , PuRhGa_5 shows a pseudogap-like suppression over a wide temperature region from T_c (7.6 K) to roughly $3T_c$ (25 K). Because of this remarkable observation, we proposed the two-component spin-fermion model and argued that the magnetic spin gap originates on the local spins of the $5f$ electrons of Pu and that the concomitant formation of the FPG (Δ_{FPG}) can provide a consistent explanation of these phenomena.

We argued previously^{3,4} that PuCoGa_5 bridges the heavy fermion superconductors and high- T_c cuprates in terms of the superconducting pairing mechanism. The observation of the pseudogap phenomenon in PuRhGa_5 and its temperature range of over two times T_c (or roughly 15 K) is another evidence that PuMGa_5 is indeed the missing link between heavy fermion superconductors and cuprates, holding the key in-

gradient – magnetic correlations – yet with an intermediate energy scale. To test and confirm this hypothesis, we propose systematic studies of the alloy system $\text{Pu}(\text{Co,Rh})\text{Ga}_5$. It will be an ideal system for further studies because it can be cleanly tuned to explore the magnetic phase diagram sketched in Fig. 5 without changing the carrier density in contrast to the high- T_c cuprates.

V. ACKNOWLEDGEMENTS

We thank John Sarrao, Joe Thompson, David Pines and Eric Bauer for many stimulating discussions. Y. B. was supported

by the KOSEF through the CSCMR and the Grant No. KRF-2005-070-C00044. This research was supported by the U.S. Department of Energy at Los Alamos National Laboratory under contract No. W-7405-ENG-36.

-
- ¹ J. L. Sarrao, L. A. Morales, J. D. Thompson, B. L. Scott, G. R. Stewart, F. Wastin, J. Rebizant, P. Boulet, E. Colineau, and G. H. Lander, *Nature* (London) **420**, 297 (2002).
 - ² F. Wastin, P. Boulet, J. Rebizant, E. Colineau, and G. H. Lander, *J. Phys.: Condens. Matter* **15**, S2279 (2003).
 - ³ N. J. Curro, T. Caldwell, E. D. Bauer, L. A. Morales, M. J. Graf, Y. Bang, A. V. Balatsky, J. D. Thompson, and J. L. Sarrao, *Nature* (London) **434**, 622 (2005).
 - ⁴ Y. Bang, A. V. Balatsky, F. Wastin, and J. D. Thompson *Phys. Rev. B* **70**, 104512 (2004)
 - ⁵ E. D. Bauer, J. D. Thompson, J. L. Sarrao, L. A. Morales, F. Wastin, J. Rebizant, J. C. Griveau, P. Javorsky, P. Boulet, E. Colineau, G. H. Lander, and G. R. Stewart *Phys. Rev. Lett.* **93**, 147005 (2004)
 - ⁶ H. Sakai, Y. Tokunaga, T. Fujimoto, S. Kambe, R. E. Walstedt, H. Yasuoka, D. Aoki, Y. Homma, E. Yamamoto, A. Nakamura, Y. Shiokawa, K. Nakajima, Y. Arai, T. D. Matsuda, Y. Haga, and Y. Ōnuki, to appear in *J. Phys. Soc. Jpn.*
 - ⁷ K. Magishi, Y. Kitaoka, G.-q. Zheng, K. Asayama, T. Kondo, Y. Shimakawa, T. Manako, and Y. Kubo *Phys. Rev. B* **54**, 10131-10142 (1996).
 - ⁸ Y. Bang, I. Martin, and A. V. Balatsky *Phys. Rev. B* **66**, 224501 (2002)
 - ⁹ Y. Bang, M. J. Graf, A. V. Balatsky, and J. D. Thompson, *Phys. Rev. B* **69**, 014505 (2004); Y. Bang, M. J. Graf, and A. V. Balatsky, *Phys. Rev. B* **68**, 212504 (2003).
 - ¹⁰ P. J. Hirschfeld, D. Vollhardt, and P. Wölfle, *Solid State Commun.* **59**, 111 (1986); P. J. Hirschfeld, P. Wölfle, and D. Einzel, *Phys. Rev. B* **37**, 83 (1988).
 - ¹¹ S. Schmitt-Rink, K. Miyake, and C. M. Varma, *Phys. Rev. Lett.* **57**, 2575 (1986).
 - ¹² H. Monien, K. Scharnberg, and D. Walker, *Solid State Commun.* **63**, 263 (1987).
 - ¹³ V. A. Sidorov, M. Nicklas, P. G. Pagliuso, J. L. Sarrao, Y. Bang, A. V. Balatsky, and J. D. Thompson, *Phys. Rev. Lett.* **89**, 157004 (2002).
 - ¹⁴ T. Mito, S. Kawasaki, Y. Kawasaki, G. -q. Zheng, Y. Kitaoka, D. Aoki, Y. . Haga, and Y. Ōnuki, *Phys. Rev. Lett.* **90**, 077004 (2003).
 - ¹⁵ S. Kawasaki, T. Mito, G.-q. Zheng, C. Thessieu, Y. Kawasaki, K. Ishida, Y. Kitaoka, T. Muramatsu, T. C. Kobayashi, D. Aoki, S. Araki, Y. Haga, R. Settai, and Y. Ōnuki, *Phys. Rev. B* **65**, 020504 (2002).
 - ¹⁶ See for example: P. Monthoux, A.V. Balatsky and D. Pines, *Phys. Rev. B* **46**, 14803, (1992).
 - ¹⁷ S. Sachdev, A. V. Chubukov, and A. Sokol, *Phys. Rev. B* **51**, 14874-14891 (1995); Y. L. Liu and Z.B. Su, *Phys. Lett. A* **200**, 393-398 (1995).
 - ¹⁸ We assume that the AFM correlation in PuMGa_5 is 2D like because the band calculations and the crystal structure of PuMGa_5 compounds, isostructural to CeMCo_5 compounds, indicate the 2D character of the electronic properties.
 - ¹⁹ A. Sokol and D. Pines, *Phys. Rev. Lett.* **71**, 2813 (1993).
 - ²⁰ S. Chakravarty, B.I. Halperin, and D.R. Nelson, *Phys. Rev. B*, **39**, 2344 (1989).
 - ²¹ N.J. Curro et al., *Phys. Rev. B* **56**, 877 (1997).
 - ²² J. Schmalian, D. Pines, and B. Stojkovic *Phys. Rev. Lett.* **80**, 3839-3842 (1998); A.P. Kampf and J. R. Schrieffer, *Phys. Rev. B* **42**, 7967 (1990)
 - ²³ P. Javorsky, E. Colineau, P. Boulet, F. Wastin, J. Rebizant, unpublished.
 - ²⁴ H. Yasuoka, (private communication).
 - ²⁵ N.J. Curro, B.-L. Young, J. Schmalian, D. Pines, *Phys. Rev. B*, **70**, 235117 (2004).
 - ²⁶ N.J. Curro et al., *Phys. Rev. Lett.* **90**, 2272002 (2003).
 - ²⁷ N.J. Curro et al., *Phys. Rev. B* **64**, 180514 (2001).
 - ²⁸ E. Kim, M. Makivic, and D. Cox, *Phys. Rev. Lett.* **75**, 2015 (1995).
 - ²⁹ P. G. Pagliuso et al., *Physica B*, **312-313**, 129 (2001).